



## A comparison of AA2024 and AA7150 subjected to ultrasonic shot peening: Microstructure, surface segregation and corrosion



Qingqing Sun<sup>a,b</sup>, Xingtao Liu<sup>a</sup>, Qingyou Han<sup>a,\*</sup>, Jie Li<sup>b</sup>, Rong Xu<sup>c</sup>, Kejie Zhao<sup>c</sup>

<sup>a</sup> School of Engineering Technology, Purdue University, West Lafayette, IN 47907, United States

<sup>b</sup> School of Chemistry and Chemical Engineering, Central South University, Changsha, Hunan 410012, China

<sup>c</sup> School of Mechanical Engineering, Purdue University, West Lafayette, IN 47907, United States

### ARTICLE INFO

#### Keywords:

AA2024

AA7150

Ultrasonic shot peening

Surface nanocrystallization

Surface segregation

Corrosion

### ABSTRACT

The influence of ultrasonic shot peening (USSP) on microstructure, surface segregation, localized and electrochemical corrosion of AA2024 was investigated using immersion test, OCP, EIS, polarization, XRD and SEM-EDS methods. The results are compared with those of AA7150. Like AA7150, second phase particles of AA2024 peened surface layer dissolved into Al matrix due to the extended solid solubility caused by USSP. After USSP, corrosion rate of AA2024 increased by 2–3 times due to surface contamination, however, intergranular corrosion (IGC) resistance of AA2024 is significantly enhanced by USSP treatment. The improvement in localized corrosion resistance is mainly attributed to grain refinement and microstructure homogenization. As opposed to AA7150, OCP of AA2024 in 3.5 wt% NaCl solution (pH = 5.8) shifts to more noble direction after USSP. This is due to the different surface segregation behaviours of the two studied alloys. The mechanism of surface segregation is also briefly discussed.

### 1. Introduction

Surface mechanical attrition treatment (SMAT) is one technique that can induce severe plastic deformation (SPD) on the surface of alloys, resulting in a strain hardening, grain refinement and induction of compressive stress [1–3]. Ultrasonic shot peening (USSP) is a relative novel method of SMAT to achieve surface SPD. There is a significant body of research regarding the corrosion properties of alloys subjected to SMAT/USSP. However, due to the complex nature of corrosion, both beneficial and deleterious effects caused by SMAT have been reported. For instance, beneficial effects of SMAT/SPD on corrosion rate of Al alloys were reported by several researchers [4–6]. However, Mustafa Abdulstaar [7], R.A. Waikar [8] and M. Navaser [9] reported that SMAT deteriorated corrosion resistance of Al alloys. The effect of SMAT on corrosion performance varies with alloy system [10,11], grain orientation [4], corrosive environment [12], temperature [13], impact parameters [14] and etc.

A detailed understanding of corrosion behavior observed for surface nanocrystallization processed materials is, however, lacking [15]. Briefly, two critical aspects in corrosion research of surface nanocrystallization processed materials have long been ignored. The first one is the localized corrosion nature of many alloys. Compared with uniform corrosion, localized corrosion, such as pitting, IGC and SCC, are more

common and more dangerous for Al alloys, especially for 2000 and 7000 series ultra-high strength Al alloys. Therefore, corrosion depth, rather than corrosion rate which can be easily derived from electrochemical curves, deserves more attention from researchers. Unfortunately, most of the published work only studied corrosion rate using electrochemical methods [7–13,16–21]. Only a few authors noticed this and measured corrosion depth in their work [4,5]. Another frequently ignored aspect is the galvanic corrosion interaction. After SPD processing, especially after surface SPD treatment, the electrochemical potential of the new formed layer of alloy changed, due to segregation of elements [22], grain refinement [1,2,23] and redistribution of elements at grain boundaries and in the matrix [24], change of passive oxide film [13] and sometimes, foreign impurities induced [22]. The potential difference between nanocrystalline surface layer and interior will, definitely, result in electron transfer and galvanic corrosion.

Previous work [22,25] has investigated the effects of USSP on electrochemical and localized corrosion of AA7150. In this work, surface nanocrystallization, surface contamination and surface segregation of AA2024 and AA7150 caused by USSP were reported and compared, and their influences on corrosion behaviours of these two aircraft alloys were studied and compared using XRD, SEM, immersion, OCP, EIS and polarization methods.

\* Corresponding author.

E-mail address: [hanq@purdue.edu](mailto:hanq@purdue.edu) (Q. Han).

**Table 1**  
Compositions of AA2024 and AA7150 (wt%).

Alloys	Zn	Mg	Cu	Mn	Si	Fe	Cr	Zr	Others	Al
AA2024	0.13	0.57	4.6	0.57	0.08	0.19	0.01	0.00	0.11	Balance
AA7150	6.5	2.3	2.3	0.1	0.12	0.15	0.04	0.10	0.21	Balance

## 2. Experimental

### 2.1. Materials and USSP setup

AA2024 was a rolled plate, received from Kaiser Aluminum Corp. and treated with temper T351. AA7150 plate was received from Alcoa Corp., rolled and treated with T7751 aging process. The compositions of the two studied alloys are listed in Table 1. The main alloying elements are Al-Mg-Cu for AA2024, while the main alloying elements are Al-Zn-Mg-Cu for AA7150. The USSP setup and parameters are described elsewhere [22].

### 2.2. Intergranular corrosion test

According to ASTM standard, G110-9257 g/L NaCl + 10 mL/L H<sub>2</sub>O<sub>2</sub> was chosen as testing solution for corrosion depth. The exposure was conducted at room temperature for 24 h, in a vessel holding 15 mL of testing solution per square cm of specimen surface area. After exposure, each specimen was rinsed with water and the cross-section of the exposure surface was etched with Keller' reagent. The maximum corrosion depth of more than 15 images (each image was 2.679 mm in length and corresponded to a maximum depth) was measured. Then the average value of maximum corrosion depths and the maximum depth of all the obtained images was calculated and compared for the untreated and USSPed alloys. The untreated represents specimen without USSP treatment but receives the same treatment prior to USSP.

### 2.3. XRD and SEM

XRD patterns were performed using a Bruker D-8 Focus X-ray diffractometer with CuK<sub>α</sub> radiation and at a 2θ scanning rate of 4°/min to determine the phase constituents in the surface layer. β<sub>hkl</sub>, which is full width at half maximum (FWHM), was determined using Jade software (MDI JADE 7 Materials Data XRD Pattern Processing, Identification, and Quantification). The value of β<sub>hkl</sub> can be described by Eq. (1) [26], from which the values of mean microstrain and nanocrystalline grain

size can be derived.

$$\beta_{\text{hkl}}^2 - \beta_0^2 = \left( \frac{K \lambda}{D_{\text{hkl}} \cos \theta} \right)^2 + (4\epsilon \tan \theta)^2 \quad (1)$$

where  $K$  is a numerical factor frequently referred to as the crystallite-shape factor ( $K = 0.89$  for Al),  $\lambda$  is the wavelength of incident wave,  $D_{\text{hkl}}$  is the crystallite size in the direction perpendicular to the lattice planes,  $hkl$  are the Miller indices of the planes being analysed, and  $\theta$  is the Bragg angle,  $\epsilon$  is microstrain,  $\beta_0$  is the instrumental broadening.

The cross-section of the peened specimen, etched by Keller's reagent (containing 95 mL of reagent water, 2.5 mL of nitric acid (70%), 1.5 mL of hydrochloric acid (37%) and 1.0 mL of hydrofluoric acid (48%)), were characterized by Phenom Desktop scanning electron microscopy (SEM) using BSE mode. Energy dispersive X-ray spectroscopy (EDS) line and mapping scan were performed to characterize surface elements segregation and surface contamination phenomena of alloys after USSP treatment.

### 2.4. Electrochemical test

A VersaSTAT 3 potentiostat/galvanostat connected to a three-electrode cell was used for the electrochemical measurements. The working electrode was the test material with an immersed area of 1.0 cm<sup>2</sup>. Platinum gauze and saturated calomel (SCE) electrodes were used as the counter and reference electrodes, respectively. Electrochemical tests were performed in naturally aerated 3.5 wt% NaCl solution. Open circuit potential (OCP) - time curves were measured for alloys subjected to USSP and 1 month natural aging treatments. Electrochemical impedance spectroscopy (EIS) measurements were conducted when OCP was stable, with the frequency ranging from 100 kHz to 0.1 Hz and the amplitude of the sinusoidal potential signal was 10 mV with respect to the OCP. Polarization curves were obtained at a scan rate of 0.2 mV/s, ranging from  $-0.3 V_{\text{OCP}}$  to  $0.3 V_{\text{OCP}}$ . All electrochemical tests were performed under room temperature in a faraday cage. To ensure the reproducibility of the results, experiments were repeated at least three times under the same experimental condition.

## 3. Results

### 3.1. Microstructure

Cross-sectional SEM backscattered electron images of AA2024 without and with USSP treatment are shown in Fig. 1a and b respectively. The original grain size of the rolled plate was 50–100 μm wide. The thickness of the USSP

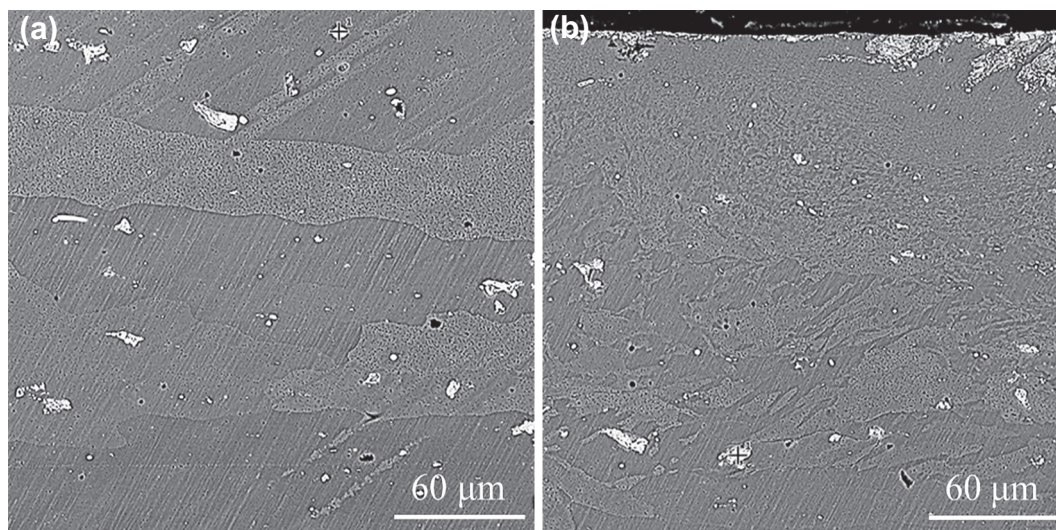


**Fig. 1.** Cross-sectional SEM backscattered electron images of AA2024: (a) as-received; (b) USSP treated.

Download English Version:

<https://daneshyari.com/en/article/8024435>

Download Persian Version:

<https://daneshyari.com/article/8024435>

[Daneshyari.com](https://daneshyari.com)